Braneworld inflation with an effective α-attractor potential

Nur Jaman[1,*] and Kairat Myrzakulov[2,†]
[1]Centre for Theoretical Physics, Jamia Millia Islamia, New Delhi-110025, India
[2]Center for Theoretical Physics, Eurasian National University, Astana 010008, Kazakhstan

(Received 8 December 2018; published 16 May 2019)

In this paper, we study inflation in the α-attractor framework with an exponential potential in the Randall-Sundrum (RS) braneworlds, where high-energy corrections to the Friedmann equation facilitate a slow roll. In this scenario, we numerically investigate the inflationary parameters and show that the high-energy brane corrections have a significant effect on the parameter α; namely, the lower values of the parameter are preferred by observation in this limit. The latter substantially reduces the tensor-to-scalar ratio of perturbations, making the RS braneworld inflation compatible with observation. We also point out that sub-Planckian values of the field displacement can be achieved by suitably constraining the brane tension.

DOI: 10.1103/PhysRevD.99.103523

I. INTRODUCTION

In the standard framework, a slowly rolling scalar field *à la* a shallow field potential may account for inflation [1]. A slow roll along a steep potential is also possible due to Hubble damping caused by high-energy brane corrections. Indeed, in the braneworld scenario, our four-dimensional space-time dubbed brane is supposed to be embedded in a higher-dimensional bulk [2,3] such that the Einstein equations on the brane are modified. The corresponding Friedmann equation includes an extra term [4,5], quadratic in density, which facilitates a slow roll in the high-energy regime at early times even in the case of a steep potential [6–9]. Thus, the braneworld scenario allows a steep potential to support inflation [10–12], which is not possible in the standard case.

In standard cosmology, an exponential potential [13] does not give viable inflationary and postinflationary behavior. The situation changes significantly in the braneworld case [10–12]. However, the steep braneworld inflation gives a ratio of tensor-to-scalar perturbation, r, around 0.4 for 60 e-folds of inflation [12,14], which is not tenable observationally [15–18]. A similar problem in standard cosmology can successfully be addressed in the α-attractor scenario [19–24]. In this framework, the kinetic term in the Lagrangian has a specific noncanonical form. The canonicalization of such a term gives rise to some flat regions or plateaus in the potential [19–22] which are suitable for the study of inflation favored by observational data [15–18]. This feature can also be suitable for the study of late time behavior, namely, quintessence [20–22,25–31].

It should be mentioned here that a super-Planckian displacement of the scalar field may spoil the flatness of the quintessential region of the potential and may generate an unwanted fifth-force problem [20–22,32]. On the other hand, it is impossible to evolve to quintessence starting from the inflationary region without invoking super-Planckian values of the field and not making the potential too curvy during inflation [33]. The α-attractor solves this problem; namely, the canonicalization of the potential makes it possible for the canonical scalar field to have a super-Planckian excursion while keeping its noncanonical counterpart under sub-Planckian.

In view of the aforesaid, we are led to consider the α-attractor construct in the framework of Randall-Sundrum (RS) braneworlds [3], which might give new insights related to the sub-Planckian nature of the noncanonical field.[1]

The structure of this paper is as follows. In Sec. II, we discuss how we obtain our effective α-attractor potential and suggest some approximations to check for analytical behavior. In Sec. III, we put the effective potential on a

*nurjaman@ctp-jamia.res.in
†kmyrzakulov@gmail.com

[1]Let us emphasize that, in the RS scenario, the TeV scale associated with the electroweak scale has a significance. Since the LHC did not see new excitations around this scale *à la* Kaluza Klein and no deviations to Newtonian potential were seen at the submillimeter scale, one could think that the scenario is ruled out. We should, however, remember, that the requirement of TeV is inspired by the naturalness problem. Let us note that the standard model of electroweak interactions is also plagued with the naturalness problem [34]; in that case, we think that there is some unknown UV completion mechanism required to tackle the issue. Thus, in the RS scenario the fundamental scale could well be higher than 1 TeV, and we can still use the scenario using similar reasoning.

brane and perform a full numerical study of different parameters related to inflation. Numerical analysis is done because of the complexity in solving the problem analytically. In this section, we also show some important features our model exhibits. Next, in Sec. IV, we show some approximated analytical results for our model. Next, in Sec. V, we compare our results with current observational bounds, and, with the results obtained, we constrain our different model parameters, especially the parameter α. Next, in Sec. VI, we briefly discuss the late time behavior followed by conclusions in Sec. VII.

II. THE EFFECTIVE α-ATTRACTOR MODEL

Considering the formal α-attractor Lagrangian density with an exponential potential in four-dimensional spacetime [19–22][2]

$$\mathcal{L} = \frac{\frac{1}{2}(\partial\phi)^2}{(1-\frac{\phi^2}{6\alpha m_p^2})^2} + V_0 e^{-\kappa\phi/m_p}, \tag{1}$$

where $\alpha > 0$ is a parameter featuring a pole in the kinetic energy, $m_p = \frac{1}{\sqrt{8\pi G}}$ is the four-dimensional reduced Planck mass, G is Newton's constant, κ is the parameter determining the steepness of the potential, and V_0 is a constant with the dimension of energy density. The modulus value of ϕ will remain less than $\sqrt{6\alpha}m_p$ for any finite value of α, because the kinetic energy becomes singular at this value. This allows the scalar field to remain under sub-Planckian values as long as $\alpha \lesssim 1/6$. The same theory can be described in terms of a canonicalized inflaton field φ related to the noncanonical scalar field ϕ via the transformation

$$\phi = \sqrt{6\alpha}m_p \tanh\left(\frac{\varphi}{\sqrt{6\alpha}m_p}\right). \tag{2}$$

From Eq. (2), it is clear that the canonical field φ can take any value, keeping the noncanonical ϕ sub-Planckian. By this transformation, the potential given in Eq. (1) is described now in terms of the canonical field of the form

$$V(\varphi) = V_0 e^{-\kappa\sqrt{6\alpha}\tanh(\frac{\varphi}{\sqrt{6\alpha}m_p})}. \tag{3}$$

This potential corresponds two plateaus; see Fig. 1. The inflationary regime featured by a plateau corresponds to $\phi \to -\sqrt{6\alpha}m_p$, or, equivalently, by $\varphi \to -\infty$, and the other plateau is featured by $\phi \to \sqrt{6\alpha}m_p$, or, equivalently, by $\varphi \to \infty$, featuring quintessence. For the inflationary limit potential, Eq. (3) becomes

[2]In Refs. [20,21], a negative cosmological constant is considered in the Lagrangian to make the vacuum energy density of the Universe zero, but we do not consider this here as its contribution is insignificant during inflation.

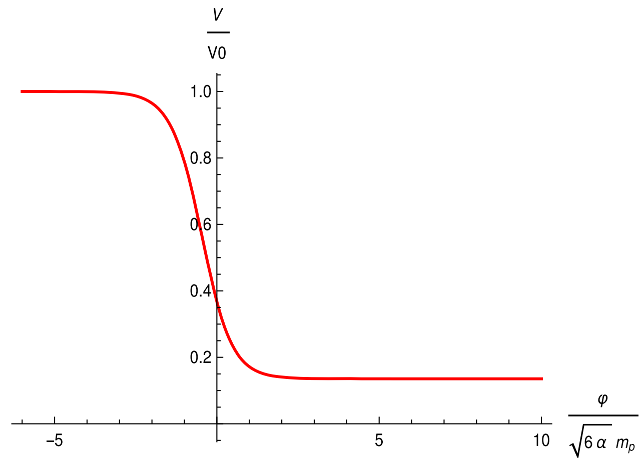

FIG. 1. Potential of the α-attractor after canonicalization (3) (n is taken to be 1).

$$V(\varphi) = M^4 \exp\left(-2ne^{\frac{2\sqrt{8\pi}}{\sqrt{6\alpha}M_{\rm Pl}}\varphi}\right), \tag{4}$$

where $M^4 = V_0 e^{\kappa\sqrt{6\alpha}}$ is a constant representing the energy scale for inflation, M has the dimension of mass, $M_{\rm Pl} \equiv m_p\sqrt{8\pi}$ is the four-dimensional Planck mass, and $n \equiv \kappa\sqrt{6\alpha}$.

III. THE EFFECTIVE α-ATTRACTOR POTENTIAL IN THE BRANEWORLD SCENARIO

We place our effective potential on the Randall-Sundrum II (RSII) brane [3] to study the inflationary scenario. The matter fields are confined to the brane only for the RSII model, so our scalar field will remain on the brane only. For a flat Friedmann-Lemaître-Robertson-Walker background on the brane with a zero four-dimensional cosmological constant, the Friedmann equation becomes [4,10,11,14]

$$H^2 \equiv \left(\frac{\dot{a}}{a}\right)^2 = \frac{8\pi}{3M_{\rm Pl}^2}\rho\left(1+\frac{\rho}{2\lambda}\right), \tag{5}$$

where a is the scale factor, H is the Hubble parameter, ρ is the energy density of the matter field on the brane, and λ is the 3-brane tension relating the 4D Planck mass $M_{\rm Pl}$ with 5D Planck mass M_5 via

$$\lambda = \frac{3}{4\pi}\frac{{M_5}^6}{{M_{\rm Pl}}^2}. \tag{6}$$

For high energies, the ρ^2 term become significant and plays a crucial role in the dynamics of the scalar field and, hence, of the Universe. The scalar field or the inflaton field φ, confined on the brane, satisfies the Klein-Gordon equation

$$\ddot{\varphi} + 3H\dot{\varphi} + V'(\varphi) = 0. \tag{7}$$

$V(\varphi)$ is the potential driving the inflation. The prime denotes a derivative with respect to φ. The presence of the quadratic term ρ^2 enhances the value of Hubble parameter (5), hereby gives extra friction to the scalar field (7), and makes its evolution slower. Combining Eqs. (5) and (7), one gets the evolution equation [6,14]

$$\frac{\ddot{a}}{a} = \frac{8\pi}{3M_{\rm Pl}^2}\left[(V - \dot{\varphi}^2) + \frac{\dot{\varphi}^2 + 2V}{8\lambda}(2V - 5\dot{\varphi}^2)\right]. \quad (8)$$

The inflationary condition $\ddot{a} > 0$ is reduced to the standard form $V > \dot{\varphi}^2$ for $\frac{\dot{\varphi}^2+2V}{8\lambda} \ll 1$. In the high-energy scenario, the condition becomes $2V > 5\dot{\varphi}^2$. This condition may used for characterizing the end of inflation [14], $2V(\varphi_{\rm end}) \simeq 5\dot{\varphi}^2_{\rm end}$. Using the slow-roll approximation ($V \gg \dot{\varphi}^2$, $\frac{\ddot{\varphi}}{3H\dot{\varphi}} \ll 1$), we can write Eqs. (5) and (7), respectively, as

$$H^2 = \frac{8\pi}{3M_{\rm Pl}^2}V\left(1 + \frac{V}{2\lambda}\right) \quad (9)$$

and

$$3H\dot{\varphi} + V'(\varphi) = 0. \quad (10)$$

These two equations (9) and (10) make the condition for the inflation end to be

$$\frac{V^3(\varphi_{\rm end})}{V'^2(\varphi_{\rm end})} \simeq \frac{5\lambda M_{\rm Pl}^2}{24\pi}. \quad (11)$$

The amplitudes of scalar and tensor perturbation in the RSII inflationary scenario are given, respectively, as [6,14,35,36]

$$A_S^2 = \frac{512}{75M_{\rm Pl}^6}\frac{V^3}{V'^2}\left(1 + \frac{V}{2\lambda}\right)^3\Big|_{k=aH}, \quad (12)$$

$$A_T^2 = \frac{4}{25\pi}\frac{H^2}{M_{\rm Pl}^2}F^2(x)\Big|_{k=aH}, \quad (13)$$

where

$$x = HM_{\rm Pl}\sqrt{3/(4\pi\lambda)} \simeq \sqrt{\frac{2V}{\lambda}\left(1 + \frac{V}{2\lambda}\right)}, \quad (14)$$

$$F(x) = \left[\sqrt{1 + x^2} - x^2\sinh^{-1}(1/x)\right]^{-1/2}. \quad (15)$$

The $\simeq$ is used under the slow-roll approximation. Amplitudes A_S and A_T are evaluated at the horizon exit, $k = aH$, with k being the comoving wave number. The two slow-roll parameters on the brane are given by

$$\epsilon \equiv \frac{M_{\rm Pl}^2}{16\pi}\left(\frac{V'}{V}\right)^2\frac{1 + \frac{V}{\lambda}}{(1 + \frac{V}{2\lambda})^2}, \quad (16)$$

$$\eta \equiv \frac{M_{\rm Pl}^2}{8\pi}\frac{V''}{V}\frac{1}{1 + \frac{V}{2\lambda}}, \quad (17)$$

which indicates that, in the high-energy regime ($V/\lambda \gg 1$), a slow roll is possible even if the potential is steep. The spectral indices of scalar and tensor perturbations are

$$n_S - 1 \equiv \frac{d\ln A_S{}^2}{d\ln k}\Big|_{k=aH}, \quad (18)$$

$$n_T \equiv \frac{d\ln A_T{}^2}{d\ln k}\Big|_{k=aH}. \quad (19)$$

Under slow-roll conditions, we get

$$n_S = 1 - 6\epsilon + 2\eta. \quad (20)$$

The number of e-folds during inflation is given by $\int_{t_*}^{t_{\rm end}} Hdt$, which under the slow-roll condition can be written as

$$N \simeq -\frac{8\pi}{M_{\rm Pl}^2}\int_{\varphi_*}^{\phi_{\rm end}}\frac{V}{V'}\left(1 + \frac{V}{2\lambda}\right)d\phi, \quad (21)$$

where $*$ denotes the value at the horizon exit. We define the ratio of tensor-to-scalar perturbation r as [14]

$$r \equiv 16\left(\frac{A_T^2}{A_S^2}\right). \quad (22)$$

In the high-energy limit $V/\lambda \gg 1$, one finds from Eq. (15) $F^2 \simeq \frac{3V}{2\lambda}$; using this together with the slow-roll approximation ($\rho \sim V$), and using Eqs. (9), (12), and (13), we get

$$r = \frac{M_{\rm Pl}^2}{\pi}\left(\frac{V'}{V}\right)^2\frac{1}{(1 + V/2\lambda)^2}F^2$$
$$= \frac{3M_{\rm Pl}^2}{2\pi}\left(\frac{V'}{V}\right)^2\frac{V/\lambda}{(1 + V/2\lambda)^2} \simeq 24\epsilon. \quad (23)$$

One can easily show that, in the low-energy limit ($V/\lambda \ll 1$), $r = 16\epsilon$, which is the standard expression.

To study inflation, we start with the potential (4). The condition for inflation end (11) gives

$$\frac{3\alpha M^4 M_{\rm Pl}^2}{64\pi n^2}\exp\left[-\frac{8\sqrt{\frac{\pi}{3}}\varphi_{\rm end}}{\sqrt{\alpha}M_{\rm Pl}} - 2ne^{\frac{4\sqrt{\frac{\pi}{3}}\varphi_{\rm end}}{\sqrt{\alpha}M_{\rm Pl}}}\right] \simeq 5\frac{\lambda M_{\rm Pl}^2}{24\pi}. \quad (24)$$

The total number of e-foldings of inflation is given by Eq. (21) for the high-energy limit ($\frac{V}{\lambda} \gg 1$):

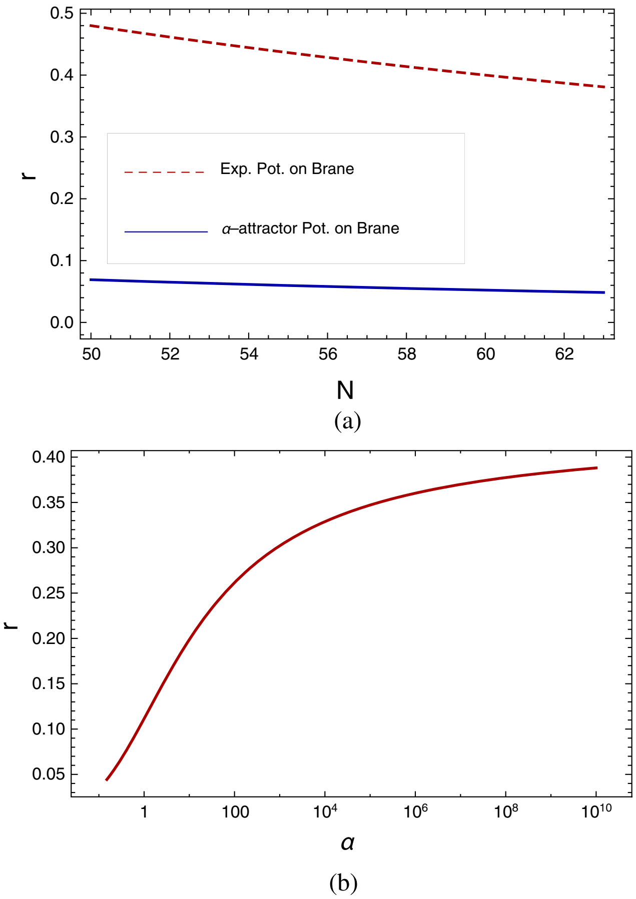

FIG. 2. The top shows the variation of r with N, the red (dashed) line for a normal exponential potential on a brane and the blue (solid) line for the exponential potential on the brane with α correction for parameter values $M^4/\lambda = 50$ and $\alpha = 0.5$. The bottom shows the asymptotic behavior of r as α increases, for $N = 55$ and $M^4/\lambda = 100$.

$$N \simeq \int_{\varphi_*}^{\varphi_{\rm end}} \frac{\sqrt{3\pi}\sqrt{\alpha}M^4}{2n\lambda M_{\rm Pl}} \exp\left[-\frac{4\sqrt{\frac{\pi}{3}}\varphi}{\sqrt{\alpha}M_{\rm Pl}} - 2ne^{\frac{4\sqrt{\frac{\pi}{3}}\varphi}{\sqrt{\alpha}M_{\rm Pl}}}\right] d\varphi. \tag{25}$$

The two slow-roll parameters in the high-energy limit become

$$\epsilon \simeq \frac{16n^2\lambda}{3\alpha M^4} \exp\left[\frac{8\sqrt{\frac{\pi}{3}}\varphi}{\sqrt{\alpha}M_{\rm Pl}} + 2ne^{\frac{4\sqrt{\frac{\pi}{3}}\varphi}{\sqrt{\alpha}M_{\rm Pl}}}\right], \tag{26}$$

$$\eta \simeq \frac{8n\lambda}{3\alpha M^4}\left(2ne^{\frac{4\sqrt{\frac{\pi}{3}}\varphi}{\sqrt{\alpha}M_{\rm Pl}}} - 1\right) \exp\left[\frac{4\sqrt{\frac{\pi}{3}}\varphi}{\sqrt{\alpha}M_{\rm Pl}} + 2ne^{\frac{4\sqrt{\frac{\pi}{3}}\varphi}{\sqrt{\alpha}M_{\rm Pl}}}\right]. \tag{27}$$

We do solve Eqs. (24) and (25) numerically, and, using (26) and (27), we compute r and n_S from the expressions (23) and (20).

The value of the tensor-to-scalar ratio r is found to be $24/N$, which is 0.4 for $N = 60$ for the standard braneworld scenario [12,14] without an α-attractor part; our numerical results show a correction for the tensor-to-scalar ratio. We found that r is depending on the ratio of potential strength M^4 to λ, i.e., $\frac{M^4}{\lambda}$ and the parameter α; it does not depend on the absolute value of M^4 and λ, which can also be seen in the crude analytical result [see Eq. (35)]. The following numerical result will confirm the fact: $r = 0.0990187$, for $\frac{M^4}{\lambda} = 100$, $\alpha = 1$, $\kappa = \sqrt{3}$ for both values of M equal to 0.1 and 0.01, respectively, where the value of λ is correspondingly chosen. Now we will discuss some important results of our analysis one by one.

(i) *N vs r*.—From Fig. 2(a), we see that we have a clear improvement for the value of r from those compared to the case of the standard exponential potential on the brane.

(ii) *Asymptotic value for α*.—In the limit $\alpha \to \infty$, α-attractor correction becomes irrelevant [19,20], and we get the usual exponential potential. From Fig. 2(b), it can be seen that r approaches its asymptotic value as we increase the value of the parameter α.

(iii) It is worth noting that the value of r is insensitive to κ in the original exponential potential, i.e., n for the potential (4), which we found to be the same from the result we obtained in the analytical approximation (35).

IV. APPROXIMATED ANALYTICAL RESULTS

An oversimplified approximation for the potential (4) can help us to get an approximate analytical result which we can use as a reference. To do so, we further simplify the potential in the limit $\varphi \to -\infty$ as

$$V(\varphi) \simeq M^4\left[1 - 2n\exp\left(\frac{2\sqrt{8\pi}}{\sqrt{6\alpha}M_{\rm Pl}}\varphi\right)\right]. \tag{28}$$

The condition for the end of inflation (11) gives

$$\frac{3\alpha M^4 M_{\rm Pl}^2 e^{-\frac{8\sqrt{\frac{\pi}{3}}}{\sqrt{\alpha}M_{\rm Pl}}\varphi_{\rm end}}}{64\pi n^2} \simeq \frac{5\lambda M_{\rm Pl}^2}{24\pi}. \tag{29}$$

The slow-roll parameters (26) and (27) under this approximation become, respectively,

$$\epsilon \simeq \frac{16\lambda n^2 e^{\frac{8\sqrt{\frac{\pi}{3}}\varphi}{\sqrt{\alpha}M_{\rm Pl}}}}{3\alpha M^4\left(1 - 2ne^{\frac{4\sqrt{\frac{\pi}{3}}\varphi}{\sqrt{\alpha}M_{\rm Pl}}}\right)^3} \simeq \frac{16\lambda n^2 e^{\frac{8\sqrt{\frac{\pi}{3}}\varphi}{\sqrt{\alpha}M_{\rm Pl}}}}{3\alpha M^4}, \tag{30}$$

$$\eta \simeq -\frac{8\lambda n e^{\frac{4\sqrt{\frac{\pi}{3}}}{\sqrt{\alpha}M_{\rm Pl}}\varphi}}{3\alpha M^4\left(1 - 2ne^{\frac{4\sqrt{\frac{\pi}{3}}\varphi}{\sqrt{\alpha}M_{\rm Pl}}}\right)^2} \simeq -\frac{8\lambda n e^{\frac{4\sqrt{\frac{\pi}{3}}}{\sqrt{\alpha}M_{\rm Pl}}\varphi}}{3\alpha M^4}. \tag{31}$$

The amplitude of the scalar perturbation (12)

$$A_S^2 \simeq \frac{M^{16}\alpha}{25\lambda^3 M_{\rm Pl}^4 n^2} e^{-\frac{8\sqrt{\frac{\pi}{3}}\varphi}{\sqrt{\alpha}M_{\rm Pl}}} \left(1-2n e^{\frac{4\sqrt{\frac{\pi}{3}}\varphi}{\sqrt{\alpha}M_{\rm Pl}}}\right)^6 \Bigg|_{k=aH}$$
$$\simeq \frac{M^{16}\alpha e^{-\frac{8\sqrt{\frac{\pi}{3}}\varphi}{\sqrt{\alpha}M_{\rm Pl}}}}{25\lambda^3 M_{\rm Pl}^4 n^2}\Bigg|_{k=aH}. \tag{32}$$

The number of e-foldings under this approximation is evaluated to be

$$N \simeq \int_{\varphi_*}^{\varphi_{\rm end}} \frac{\sqrt{3\pi}\sqrt{\alpha}M^4}{2n\lambda M_{\rm Pl}} e^{-\frac{4\sqrt{\frac{\pi}{3}}\varphi}{\sqrt{\alpha}M_{\rm Pl}}} \left(1-2n e^{\frac{4\sqrt{\frac{\pi}{3}}\varphi}{\sqrt{\alpha}M_{\rm Pl}}}\right)^2 d\phi$$
$$\simeq \int_{\varphi_*}^{\varphi_{\rm end}} \frac{\sqrt{3\pi}\sqrt{\alpha}M^4 e^{-\frac{4\sqrt{\frac{\pi}{3}}\varphi}{\sqrt{\alpha}M_{\rm Pl}}}}{2n\lambda M_{\rm Pl}} d\varphi. \tag{33}$$

Using the condition of inflation end (29), we express N in terms of the field value at the horizon exit:

$$N \simeq \frac{3\alpha M^4 \left(e^{-\frac{4\sqrt{\frac{\pi}{3}}\varphi_*}{\sqrt{\alpha}M_{\rm Pl}}} - \frac{2n\sqrt{10}\sqrt{\frac{\lambda}{\alpha}}}{3M^2}\right)}{8\lambda n}. \tag{34}$$

Using Eq. (34) and the fact that $r = 24\epsilon$, we find the tensor-to-scalar ratio from Eq. (30):

$$r \simeq \frac{288\alpha\lambda M^4}{(\sqrt{10}\sqrt{\alpha\lambda}M^2 + 4N\lambda)^2} \simeq \frac{288}{10\left(1+\frac{4N}{\sqrt{10\alpha}\sqrt{\frac{M^4}{\lambda}}}\right)^2}. \tag{35}$$

The amplitude of scalar perturbation (32) is found to be

$$A_S^2 \simeq \frac{4M^8(\sqrt{10}M^2\sqrt{\alpha\lambda} + 4\lambda N)^2}{225\alpha\lambda^3 M_{\rm Pl}^4}$$
$$\simeq \frac{8(\frac{M^4}{\lambda})^2 M^4}{45 M_{\rm Pl}^4}\left(1+\frac{4N}{\sqrt{10\alpha}\sqrt{\frac{M^4}{\lambda}}}\right)^2. \tag{36}$$

It should be mentioned here that the relations given by Eqs. (28)–(36) represent only approximate expressions for the respective quantities. We see from Eqs. (4) and (28) that this approximation breaks down for small values of φ or $\alpha < 1$, which is also confirmed by numerical results.

V. CONSTRAINING MODEL PARAMETERS FROM OBSERVATIONS

In order to constrain the parameters of our model, we stick to our numerical results. First, we find that r is independent of M and κ and depends only on the ratio $\frac{M^4}{\lambda}$ and α.

The observational constraint on the parameter, $r \lesssim 0.06$ [15,17,18], allows us to constrain the parameter α and the

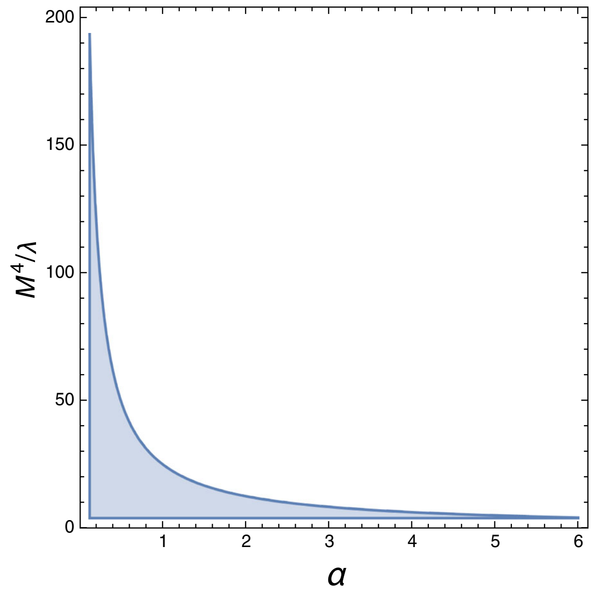

FIG. 3. allowed region for α and M^4/λ for $r \leq 0.06$.

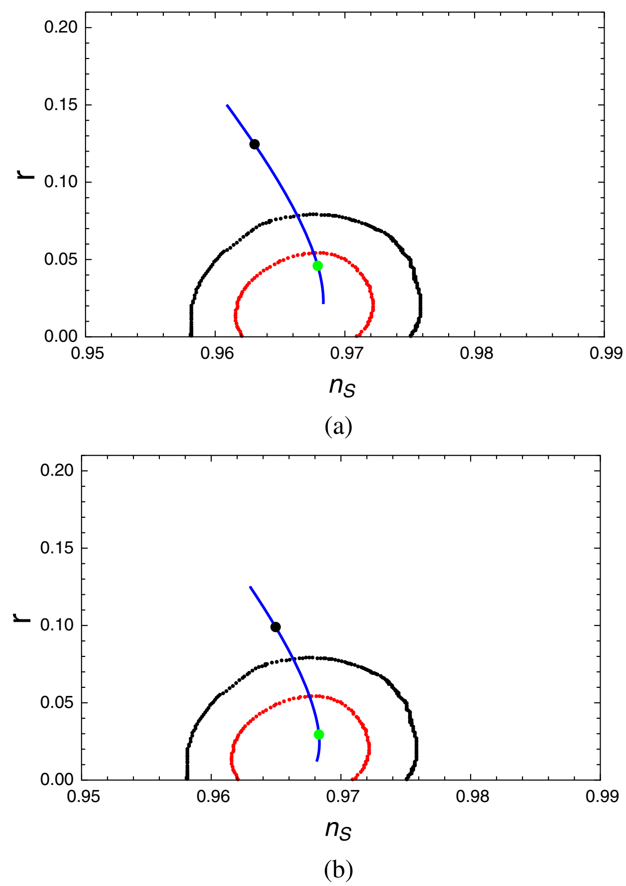

FIG. 4. The 68% (red) and 95% (black) contour regions (n_S-r plane) taken from Planck 2018 results (TT, TE, EE + lowE + lensing + BK14 + BAO) [18]; we overlay our model's result on it. We obtain our results by varying α from 0.16 to 10. For both figures, the black dot and green dot correspond to $\alpha = 5$ and 0.5, respectively. The solid blue line is for $N = 60$. For the top, $\frac{M^4}{\lambda} = 40$, and for the bottom, $\frac{M^4}{\lambda} = 20$.

TABLE I. Values of M for different α; λ is taken as allowed by r.

α	M (GeV)
0.167	1.69×10^{15}
1	4.15×10^{15}
10	1.31×10^{16}

ratio M^4/λ. Theoretically, the high-energy limit corresponds to $\frac{M^4}{\lambda} \gg 1$, but this ratio is highly dependent on the other parameter α under the observational bound. A higher value of the parameter α limits the parameter M^4/λ to a lower value, in other words, a decent limit of the assumption that during inflation $M^4/\lambda \gg 1$ pushes α to a lower value. The bound $\alpha \leq 39.6$ in Ref. [20] is reduced to $\alpha \lesssim 3.6$ for a value of $M^4/\lambda \gtrsim 7$. In Fig. 3, we show the allowed values of α against M^4/λ. In Fig. 4, we compare our results for different parameters' values with Planck 2018 results [18].

The noncanonical scalar degrees of freedom ϕ remains sub-Planckian as long as $\alpha \lesssim \frac{1}{6}$ [Eq. (2)]. We can obtain this bound in a more compelling way in our model if we consider $\frac{M^4}{\lambda} \gtrsim 150$ along with the observational bound $r \lesssim 0.06$. In other words, the value of $\frac{M^4}{\lambda}$, nearly bigger than 150, will always keep the noncanonical scalar degree of freedom within a sub-Planckian value.

The COBE normalization corresponds to the amplitude of the scalar perturbations [see Eq. (12)] $A_S \simeq 2 \times 10^{-5}$ [37], which along with the bound on α determines the energy scale of inflation. We found that (Table I) it is near the grand unification scale, almost the same as the one in standard inflationary cosmology. Consequently, after inflation ends, the field will have a large overshoot below the background freezing itself for a long time; only at late times will it evolve, mimicking cosmological-constant-like behavior.

VI. LATE TIME BEHAVIOR

Let us briefly comment on the postinflationary features of the model. First, the brane corrections to the Friedmann equation are insignificant in the postinflationary era. Second, it is interesting that, irrespective of the nature of the original exponential potential, the α-attractor effective potential (see Fig. 1) has a generic form; namely, it has a plateau followed by a sharp steep behavior like a waterfall settling fast to a constant value thereafter. In this case, the tracker [38–41] behavior is inherently absent, which makes the dynamics of the scalar field sensitive to its initial conditions. The thawing behavior in the model under consideration can be understood analytically. Actually, the important features of dynamics are encoded in a quantity dubbed Γ, which for the potential (3) is given by

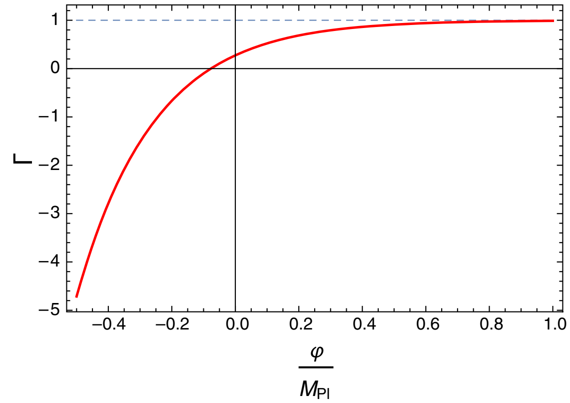

FIG. 5. The figure shows the behavior of Γ with φ, for potential (3) with a residual vacuum energy density $V_0 e^{-\kappa\sqrt{6\alpha}}$ subtracted from the standard exponential potential in (1) as taken in Refs. [20,21]; the dashed line represents a constant value 1.

$$\Gamma(\varphi) \equiv \frac{V(\varphi)'' V(\varphi)}{V(\varphi)'^2} = \frac{e^{-n}}{n}\left\{e^n - e^{n\tanh\left(\frac{2\sqrt{2\pi/3}}{M_{\rm Pl}\sqrt{\alpha}}\varphi\right)}\right\} \times \left\{n + \sinh\left(\frac{4\sqrt{2\pi/3}}{M_{\rm Pl}\sqrt{\alpha}}\varphi\right)\right\}. \tag{37}$$

Equation (37) tells us that Γ increases fast with ϕ and crosses zero and approaches unity thereafter, mimicking the exponential behavior (see Fig. 5). On the other hand, to realize tracker behavior, it is necessary that Γ being greater than unity stays close to one for a long time such that the field approximately mimics the background. In the present case, the slope of the potential, starting from a large value, gradually diminishes, pushing the system to the slow-roll regime at late times. Thus, owing to the behavior of Γ in Fig. 5, the field energy density would witness the large overshoot with respect to the background in a short span of time, freezing the field on its potential due to large Hubble damping. Field evolution would commence only at late stages when the background energy density becomes comparable to the field energy density, allowing the slow roll of a field giving rise to late time acceleration; slow roll is characterized by shallow exponential-like behavior. Hence, the present scenario gives rise to thawing behavior as noticed in Refs. [20,22].

VII. CONCLUSION

In this paper, we have considered an inflationary scenario in the α-attractor framework for an exponential potential on a RS brane. We have carried out a full numerical analysis and presented approximated analytical results. We have found that our results pass the observational constraint for suitable parameter values. The observational bound on the parameter tensor-to-scalar ratio

$r \leq 0.06$ [17,18] is easily satisfied by our model for a range of parameters—$\alpha \lesssim 3.6$ with $M^4/\lambda \gtrsim 7$. We found that a lower value of the parameter α gives rise to a large range of the parameter M^4/λ, falling within the window allowed by observations (Fig. 3). The lower bound on α, related to the inflation scale $\alpha \gtrsim 10^{-7}$ [20], is not considered here to compare with observational consistency. The significance of the brane correction underlies with the assumption that $V/\lambda \gg 1$ or, equivalently, $M^4/\lambda \gg 1$ during inflation, which automatically pushes α toward lower values in order to meet observational constraints. We numerically found that, for consistency with observation, $M^4/\lambda \gtrsim 150$ corresponds to $\alpha < 1/6$, which keeps the noncanonical scalar field to be sub-Planckian. It is worth mentioning that we do not attempt to constrain here the parameters V_0 and κ directly as done in Refs. [20,21]; however, constraining $\frac{M^4}{\lambda}$ and α puts some indirect constraints on these parameters. In Ref. [21], a rather tight bound is given on the parameter α based on the dark energy observations and the super-Planckian issue, $1.5 \leq \alpha \leq 4.2$. Our analysis is compatible with this value, as we can see from Fig. 3. We also find that our inflation scale is near the grand unification scale, the same as the case for standard inflationary models. As for the postinflationary evolution, we have argued based upon our analytical expressions that the scenario under consideration should give rise to thawing behavior; see Fig. 5 and the discussion in Sec. V noticed numerically in Refs. [20,21]. The present work, with high numerical precision, can be extended to obtain more accurate bounds on the parameters. The other aspects associated with inflation like reheating can also be investigated for the model under consideration. The investigation of alternative reheating suitable to the present framework is left for future work.

ACKNOWLEDGMENTS

N. J. is grateful to M. Sami for fruitful discussions. He is also thankful to Bikash and Safia for their help in the work. N. J is thankful to University Grants (UGC), Government of India for providing financial support through JRF. We thank Romesh Kaul for fruitful discussions.

[1] A. D. Linde, Phys. Lett. **129B**, 177 (1983); Lect. Notes Phys. **738**, 1 (2008); arXiv:astro-ph/9901124.
[2] K. Akama, Lect. Notes Phys. **176**, 267 (1982); N. Arkani-Hamed, S. Dimopoulos, and G. R. Dvali, Phys. Lett. B **429**, 263 (1998); L. Randall and R. Sundrum, Phys. Rev. Lett. **83**, 3370 (1999); A. R. Liddle and A. N. Taylor, Phys. Rev. D **65**, 041301 (2002).
[3] L. Randall and R. Sundrum, Phys. Rev. Lett. **83**, 4690 (1999).
[4] T. Shiromizu, K. i. Maeda, and M. Sasaki, Phys. Rev. D **62**, 024012 (2000).
[5] P. Binetruy, C. Deffayet, U. Ellwanger, and D. Langlois, Phys. Lett. B **477**, 285 (2000); P. Binetruy, C. Deffayet, and D. Langlois, Nucl. Phys. **B565**, 269 (2000).
[6] R. Maartens, D. Wands, B. A. Bassett, and I. Heard, Phys. Rev. D **62**, 041301 (2000).
[7] J. M. Cline, C. Grojean, and G. Servant, Phys. Rev. Lett. **83**, 4245 (1999); C. Csaki, M. Graesser, C. F. Kolda, and J. Terning, Phys. Lett. B **462**, 34 (1999); D. Ida, J. High Energy Phys. 09 (2000) 014.
[8] Y. g. Gong, arXiv:gr-qc/0005075.
[9] P. S. Apostolopoulos, N. Brouzakis, E. N. Saridakis, and N. Tetradis, Phys. Rev. D **72**, 044013 (2005).
[10] V. Sahni, M. Sami, and T. Souradeep, Phys. Rev. D **65**, 023518 (2001).
[11] M. Sami and V. Sahni, Phys. Rev. D **70**, 083513 (2004).
[12] E. J. Copeland, A. R. Liddle, and J. E. Lidsey, Phys. Rev. D **64**, 023509 (2001).
[13] F. Lucchin and S. Matarrese, Phys. Rev. D **32**, 1316 (1985).
[14] S. Tsujikawa and A. R. Liddle, J. Cosmol. Astropart. Phys. 03 (2004) 001.
[15] P. A. R. Ade *et al.* (Planck Collaboration), Astron. Astrophys. **594**, A13 (2016).
[16] P. A. R. Ade *et al.* (BICEP2 and Keck Array Collaborations), Phys. Rev. Lett. **116**, 031302 (2016).
[17] P. A. R. Ade *et al.* (BICEP2 and Keck Array Collaborations), Phys. Rev. Lett. **121**, 221301 (2018).
[18] Y. Akrami *et al.* (Planck Collaboration), arXiv:1807.06211.
[19] A. Linde, J. Cosmol. Astropart. Phys. 02 (2017) 028.
[20] K. Dimopoulos and C. Owen, J. Cosmol. Astropart. Phys. 06 (2017) 027.
[21] K. Dimopoulos, L. Donaldson Wood, and C. Owen, Phys. Rev. D **97**, 063525 (2018).
[22] Y. Akrami, R. Kallosh, A. Linde, and V. Vardanyan, J. Cosmol. Astropart. Phys. 06 (2018) 041.
[23] M. Shahalam, M. Sami, and A. Wang, Phys. Rev. D **98**, 043524 (2018).
[24] M. Shahalam, R. Myrzakulov, S. Myrzakul, and A. Wang, Int. J. Mod. Phys. D **27**, 1850058 (2018).
[25] C. García-García, E. V. Linder, P. Ruíz-Lapuente, and Miguel Zumalacárregui, J. Cosmol. Astropart. Phys. 08 (2018) 022; Phys. Rev. D **97**, 106003 (2018).
[26] P. J. E. Peebles and A. Vilenkin, Phys. Rev. D **59**, 063505 (1999).
[27] E. J. Copeland, M. Sami, and S. Tsujikawa, Int. J. Mod. Phys. D **15**, 1753 (2006).
[28] M. Wali Hossain, R. Myrzakulov, M. Sami, and E. N. Saridakis, Int. J. Mod. Phys. D **24**, 1530014 (2015).

[29] S. S. Mishra, V. Sahni, and Y. Shtanov, J. Cosmol. Astropart. Phys. 06 (2017) 045.
[30] M. Sami and N. Dadhich, arXiv:hep-th/0405016
[31] J. Rubio and C. Wetterich, Phys. Rev. D **96**, 063509 (2017).
[32] C. Wetterich, Phys. J. **3N12**, 43 (2004).
[33] K. Dimopoulos, Phys. Rev. D **68**, 123506 (2003).
[34] R. K. Kaul, arXiv:0803.0381.
[35] D. Langlois, R. Maartens, and D. Wands, Phys. Lett. B **489**, 259 (2000).
[36] B. R. Dinda, S. Kumar, and A. A. Sen, Phys. Rev. D **90**, 083515 (2014).
[37] E. F. Bunn, A. R. Liddle, and M. J. White, Phys. Rev. D **54**, R5917 (1996); E. F. Bunn and M. J. White, Astrophys. J. **480**, 6 (1997).
[38] M. Sami, arXiv:0904.3445; J. Cosmol. Astropart. Phys. 06 (2017) 045.
[39] M. Sami, Models of Dark Energy, Center for Theoretical Physics, Jamia Millia Islamia, New Delhi, India, https://www.ctp-jamia.res.in/people/models_of_dark_energy.pdf.
[40] M. Sami, arXiv:0901.0756.
[41] P. J. Steinhardt, L. M. Wang, and I. Zlatev, Phys. Rev. D **59**, 123504 (1999).